Marmara Fen Bilimleri Dergisi 2016, 1: 35-48
DOI:10.7240/mufbed.67523

Prediction of Two Bladed Horizontal Axis Wind Turbine Acoustics

A. Alper KURULTAY*, Emre ALPMAN

Marmara University, Faculty of Engineering, Department of Mechanical Engineering, 34722, Kadıköy, İstanbul

ABSTRACT

Wind power industry has been a growing market and maturing technology for several decades. Increasing wind power generation necessitates closer installation of wind turbines to people and their residences. For that reason, wind turbine noise becomes a serious and controversial phenomenon and it is anticipated to become more stringent issue while wind power generation is increased recently. The aim of this study was to propose a methodology to predict the wind turbine blade noise by using two dimensional blade section flows and noise analysis/simulation and combining the noise sources to evaluate the total blade noise with reasonable accuracy.

Within the scope of this work, the purpose was to perform a two dimensional flow and noise simulation for the two bladed NREL Phase VI wind turbine with the aid of a commercially available Computational Fluid Dynamics (CFD) software ANSYS-FLUENT by using User Defined Functions after applying some corrections under certain assumptions. Analysis results were compared with the 12% scaled model of NREL Phase VI wind turbine acoustic noise measurements conducted in In Korea Aerospace Research Institute (KARI) at the low speed wind tunnel. Blade noise of the measurements were compared with the analysis results at different wind speeds of 5.4 m/s, 7.4 m/s, 12.3 m/s, and 13.3 m/s. For the tip region and inboard area of the blade, reasonable agreement was achieved at certain wind speeds. Additionally, the summation of the contribution from the each blade section was used to predict the total noise emission.

Keywords: Wind Turbine Noise, NREL Phase VI, Aero acoustics, Computational Fluid Dynamics.

I. INTRODUCTION

Global warming and climate change lead the countries to the development of renewable and green energies. Wind power has been one of the fastest developing energy sources in the last years. Worldwide wind power generation was 6.1 GW at the end of 1996 and 369.6 GW at the end of 2014. 2014 was a record year for the wind industry as annual installations crossed the 50 GW level for the first time. By the end of 2019 it has been forecasted the total wind power generation would exceed 650 GW [1].

The governments in European Countries adopted a target to obtain 20% of electricity from renewable energy sources by 2020. Additionally, wind energy generation will increase from 82 TWh in 2006 to over 477 TWh by 2020 among European Countries based on the projected growth rates [2].

By considering the numbers, wind power industry has been a growing market and maturing technology for several decades. Additionally, wind power is increasing its share in energy industry with installed capacity [1].

Increasing wind power generation necessitates closer installation of wind turbines to people and their residences. For that reason, wind turbine noise becomes a serious and controversial phenomenon and it is anticipated to become more stringent issue while wind power generation is increased.

The wind turbines have become quieter with the advancements in technology in the last decade. Designers showed some effort to reduce noise levels in 1990s and 2000s. Since the turbine diameters get bigger, the noise levels of wind turbines get higher [3].

Some of the noise limits in various European countries are shown in Table 1 and night time noise limits in Europe and North America are tabulated in Table 2.

Even though achievements have been noted, noise limits in Table 1 and Table 2, especially in residential areas shall be considered. Wind turbine noise is still an important issue and need to be considered at the turbine installation site evaluation phase especially when close to residences. There are some studies related to wind turbine noise perception and discomfort issues in the last decade.

Sorumlu yazar/Corresponding author: A. Alper Kurultay, **Tel:** +90 (312) 496 65 42, **e-posta:** alper_kurultay@hotmail.com,
Gönderilme/ Submitted: 22.01.2016, **Kabul/Accepted:** 08.04.2016

Table 1. Noise Limits of Sound Power Levels in Various European Countries [4]

Country	Commercial	Mixed	Residential	Rural
Denmark			40 dB(A)	45 dB(A)
Germany (day)	65 dB(A)	60 dB(A)	55 dB(A)	50 dB(A)
(night)	50 dB(A)	45 dB(A)	40 dB(A)	35 dB(A)
Netherlands (day)		50 dB(A)	45 dB(A)	40 dB(A)
(night)		40 dB(A)	35 dB(A)	30 dB(A)

Table 2. Comparison Between Countries with L_{Aeq} Night-time Noise Limits Values [5]

Country / City	Residential (L_{Aeq} Night-time)	Rural (L_{Aeq} Night-time)
Belgium - Wallonia	45 dB(A)	45 dB(A)
Belgium Flanders	43 dB(A)	43 dB(A)
Denmark (8 m/s)	44 dB(A)	39 dB(A)
France	35 dB(A)	35 dB(A)
Germany	45 dB(A)	40 dB(A)
Sweden (8 m/s)	35 dB(A)	40 dB(A)
South Australia	35 dB(A)	40 dB(A)
Canada - Alberta	40 dB(A)	40 dB(A)
Canada - Ontario (8m/s)	45 dB(A)	45 dB(A)
USA - Colorado-Arapahoe Cnty	50 dB(A)	50 dB(A)
USA - Georgia	55 dB(A)	55 dB(A)
USA - Indiana - Tipton Cnty	45 dB(A)	45 dB(A)
USA - Michigan	55 dB(A)	55 dB(A)
USA - Minnesota	50 dB(A)	50 dB(A)
USA - Nevada - Lyon Cnty	55 dB(A)	55 dB(A)
USA - Wisconsin	45 dB(A)	45 dB(A)
USA - Wyoming - Laramie Cnty	50 dB(A)	50 dB(A)

According to Pederson and Waye [6], survey results with people in rural locations showed that annoyance increased with noise levels. Survey showed that annoyance increased more rapidly with wind turbines than other stationary industrial noise sources.

The study of Van Den Berg [7] revealed that noise from a 30 MW wind farm became more noticeable and disturbing to nearby residents at night. According to the study, although the noise was always present, certain aspects of turbine noise was not noticeable during the day, but became very noticeable at night.

In practice, if installation of a wind turbine is proposed within a distance of three times blade tip height to residences or any noise sensitive receptor, a noise study should be done and published [3]. In this context, wind turbine noise still a subject of discussion and discomfort.

A questionnaire was applied in United Kingdom to compare sleep and general health outcomes between participants living close to Industrial Wind Turbines (IWT) and those living away from them [8]. According to the study, industrial wind turbines' noise emissions disturbed the sleep and caused daytime sleepiness and impaired mental health in residents living in the vicinity of 1.4 km of the two wind turbines installations studied [8].

One of the most comprehensive studies about wind turbine noise and health, was performed during 2013-2014 in Canada and results were published in 2015 [9]. The study provided no linkage between exposure to wind turbine noise and any of the self reported illnesses and chronic conditions about stress and sleep as well. But on the other hand, in the study an association was found between increasing level of noise and individuals reporting to be very or extremely annoyed [9].

In the systematic review study of Schmidt and Klokker, a comprehensive literature survey was applied to more than 1200 articles. Finally 36 articles, addressing specific health related results in relation with wind turbine noise exposure, were outlined [10]. According to the study, it was logical to conclude that noise radiation by wind turbines increased the risk of annoyance and sleep disturbance on people in the vicinity. And, tolerable limit of noise was estimated to be around LAeq of 35 dB according to the study. Additionally, the study indicated that annoyance of noise and sleep disturbance were related to each other and this sleep disturbance possibly could lead to unfavorable health effects [10].

Another systematic review about the effect of the wind turbine noise on sleep and quality of life was published by Onakpaoya et al. [11]. The authors investigated experimental and observational studies about the wind turbine noise. It was concluded in the study that the exposure to wind turbine noise might be associated with increased frequency

of annoyance and sleep problems. And, the attitude of individuals toward wind turbines could influence the type of response [11].

In addition to the fact that there have been some discomfort issues about wind turbine noise, researchers from different countries and different academic institutions keep working on numerical methods for wind turbine noise prediction.

In the study of Son et al. [12], flow fields around the wind turbine blade were calculated based on an unsteady vortex lattice methods based on potential flow. Tonal noise (low frequency noise) was predicted by Farassat 1A equation; additionally semi empirical formulas were used for the prediction of broadband noise such as airfoil self noise and turbulence ingestion noise.

The properties of noise intensity function were analyzed by Guarnaccia et al. [13] from an analytical point of view, focusing on the slope of intensity function when considering different dependences. Additionally, comparison between the presented model and results of commercial noise prediction software were sketched in the study.

Tadamasa and Zangeneh [14] offered a dual methodology combining commercial CFD solver for calculation of aerodynamic noise sources and Ffowcs Williams-Hawkings (FW-H) equation for far field propagation calculation. The developed FW-H acoustic codes were applied to calculate the noise radiated from NREL (National Renewable Energy Laboratory) Phase VI wind turbine blades.

Since wind turbine noise is still an important issue especially when sited close to residential areas, numerical methods for noise prediction shall be generated and validated. Then, the proposed models shall be used to alter wind turbine (i.e.airfoil) geometry for wind turbine noise reduction. It is well known that inflow turbulence and yaw error directly affects the performance of wind turbines [15]. Since the performance is related to the pressure distribution over the blades, the acoustic signature of the turbine will also be considerably affected due to those effects. According to the work of Simss et al. [16] performed by NREL, UAE field testing showed that wind turbines operate in very complex environmental conditions. According to the study, quickly-changing wind velocity, rapidly-shifting wind directions, and widely varying levels of turbulence and shear were contributing factors in the environment [16].

In the study of Katinas et al. [17], measurements were performed and noise propagation models were applied. The authors concluded that the biggest change occurred in noise spectrum between 200 Hz and 5000 Hz. Only insignificant changes were observed in infrasound, low frequency (16-200 Hz), and ultrasound frequency ranges. Moreover, wind turbine noise was concealed by the background noise above 10 m/s wind velocities according to the study [17].

Airfoil optimization for low noise and high performance was conducted in typical three bladed 10 kW wind turbine considering six different airfoils in the study of Göçmen and **Özerdem** [18]. The authors used XFOIL as flow analysis tool and semi empirical noise model NAFNoise as self noise analysis tool. The outcomes of the study revealed higher lift to drag ratios and decreased noise emission levels up to 5 dB [18].

Lee and Lee [19] studied the generated noise of a small wind turbine numerically and experimentally. They conducted numerical predictions of turbulence ingestion noise, turbulent boundary layer trailing edge noise, and trailing edge bluntness noise based on previously proposed semi empirical formulae. The prediction results were compared with field measurement data. It was concluded for small with turbine that the trailing edge bluntness noise could be a dominant noise source unless the blades of wind turbine had very sharp trailing edge [19].

The study of Ramirez and Wolf [20] aimed to analyze the effects of trailing edge bluntness over a NACA 0012 airfoil tonal noise for low to moderate Mach numbers. The combined approach was utilized in the study such as direct calculation for near field source computations and Ffowcs-Williams Hawkings equation as the acoustic analogy formulation [20].

As stated in previous works of different research institutes and governmental offices, aerodynamic noise radiated from the wind turbine generates discomfort to the neighboring residences due to the closer wind farm installation and 24 hours a day noise generation. In order to reduce the public disturbance, there needs to be more research and development performed to define how wind turbine noise is generated and how it can be controlled and reduced.

With the aid of the computer technologies, noise source modeling improvement can help in order to gain insight to the correct behavior of the generated noise by the wind turbine. There is a strong need to develop noise prediction methods and to find noise reducing concepts for wind turbines to be able to further expand wind turbine installation sites. It is expected the more studies for the prediction and the evaluation of noise generated by the wind turbine will be required.

The aim of this study was to propose a methodology to predict the wind turbine blade noise under steady conditions by using two dimensional blade section flow and noise

analysis/simulations and by combining the noise sources to evaluate the total blade noise with reasonable accuracy.

II. THEORETICAL BACKGROUND

Noise generated by wind turbine is evaluated using the Lighthill's acoustic analogy and Ffowcs Williams and Hawkings (FW-H) equation.

In acoustic analogy, it is assumed that the acoustic fluctuations are small enough in such a way that they do not have any effect on the mean aerodynamic flow. When this assumption is reasonably satisfied it is possible to perform a combined double analysis; a Computational Fluid Dynamics (CFD) analysis for the mean aerodynamic flow, and an acoustic analysis for acoustic quantities.

2.1 Ffowcs Williams and Hawkings (FW-H) equation

The FW-H equation is the most general form of the Lighthill's acoustic analogy and it has been utilized to predict the noise generated by complex arbitrary motions. The original FW-H equation was developed in 1969 from Lighthill's acoustic analogy [21] by including the effect of the moving solid body [22].

In FW-H equation the Navier Stokes (momentum) equations are rearranged into the form of an inhomogeneous wave equation with monopole and dipole sources on the body surface and with a quadrupole source distribution in the volume surrounding the body [23].

It is first derived by representing the blade surface as moving control surface, which introduces discontinuity in the unbounded fluid domain. It has been assumed that the flow inside this control surface have the same fluid state as the undisturbed medium and outside as the real state including the influence from the body. FW-H equation in differential form is given below by assuming no fluid flow through the control surface [23].

$$\frac{1}{c_o^2}\frac{\partial^2 p'}{\partial t^2} - \overline{\nabla^2} p' = \frac{\partial}{\partial t}[(\rho_o v_n)\delta(f)] - \frac{\partial}{\partial x_i}[l_i \delta(f)] + \frac{\overline{\partial^2}}{\partial x_i \partial x_j}[T_{ij} H(f)] \quad (1)$$

Where c_o is the speed of sound in undisturbed medium, $p'$is the acoustic pressure $p' = c_o^2(\rho - \rho_o)$, v_n is the local normal velocity of the integration surface, p_{ij} is the compressive stress tensor that includes the surface pressure and viscous stress, $l_i = p'_{ij} n_j$ is the local force vector components exerted by the surface on fluid, (the force intensity (force/ unit area) acting on the fluid) $T_{ij} = \rho u_i u_j + p_{ij} - c_o^2 \rho \delta_{ij}$ is the Lighthill stress tensor. $\delta(f)$ and $H(f)$ are the Dirac delta and the Heaviside functions, respectively.

As a summary, the three source terms on the right hand side of FW-H equation are known as the thickness, loading and quadrupole source terms, respectively. This terminology is proper if only data surface corresponds to a solid (impermeable) surface [23]. The computation of the quadrupole contribution requires volume integration of the entire source region and can be difficult to implement. The details of each source terms were given in the studies of Tadamasa and Zangeneh [24], and Filios et al. [25].

It is known that the quadrupole sources are responsible for distortion of the acoustic wave form, hence noise generation. The studies of Di Francescantonio [26], Brentner and Farassat [27] showed that the surface source terms of the FW-H equation account for the nonlinear quadrupole terms surrounded by a permeable integration surface. The most intense quadrupole sources were in the vicinity of the blades.

In the study of Brentner and Farassat [27] it was shown that if surface surrounds the blade and the volume of intense quadrupole sources in the FW-H method, then the level of acoustic pressure could be accurately calculated. The weaker quadrupole sources, which are distant from the blade surface, make smaller distortion of the acoustic wave form. For that reason, the external quadrupole sources might be ignored when the integration surface is quite close to the noise generating surface.

One of the recent studies done by Rahier et.al. [28] provided insight to the additional terms for the use of FW-H surface integrals. The study specified the links between the surface and volume integrals. Additionally, the writers defined a new expression of additional surface terms that could represent an estimate of the missing volume integral [28].

III. METHODOLOGY

Wind Tunnel Test Configurations performed and published by National Renewable Energy Laboratory (NREL) in Unsteady Aerodynamics Experiment (UAE) Phase VI [29]. The results of these experiments have been one of the most comprehensive tests about wind turbine aerodynamics. Therefore, a series of wind tunnel tests were carried out in Korea Aerospace Research Institute (KARI) for the study of the scaled effect of wind turbine model. In KARI, 12% scaled model of NREL Phase VI wind turbine was tested at the low speed wind tunnel. Also, KARI conducted acoustic noise measurement with 144 channel microphone array. The wind turbine was operated at a constant rotating speed of 600 rpm to match the tip Mach number of real model test at NASA Ames wind tunnel [30].

Within the scope of this work, the purpose was to perform a two dimensional flow and noise simulation for the two bladed NREL Phase VI wind turbine with the aid of a commercially available Computational Fluid Dynamics (CFD) software ANSYS-FLUENT [31] by using User Defined Functions after applying some corrections under certain assumptions.

Numerous two dimensional simulations were made to gain information about different aspects of the noise generating mechanism of the flow around NREL Phase VI [29] turbine blade. Primarily, numerical/simulation results were compared with the NREL Phase VI experimental data [30] for validation; second, observations were made to draw some conclusions to check the sufficiency of the numerical results.

3.1. Turbine Geometry

The turbine had a stall regulated rotor and had a rated power of 19.8 kW with two twisted and tapered blades based on the S809 airfoil [32] with a diameter of 10.1 m. Rotor rotated at an angular speed of 72 rpm. Details about the blade geometry are available in reference [29].

3.2. Computational Domain and Grid

Two dimensional S809 airfoil model and mesh was generated by using GAMBIT mesh generator. Domain size was 30 chord length in longitudinal axis, 20 chord length in vertical axis. Leading edge of the airfoil was stationed 10 chord lengths far from the inlet and 20 chord lengths far from the outlet. In vertical direction, the airfoil was stationed in the symmetry axis.

An elliptical surface was defined around the airfoil. Structured mesh was applied inside the ellipse; mapped mesh was applied at the outer field of the ellipse. Finer mesh was applied around the airfoil.

Boundary conditions of the domain were chosen as follows; velocity inlet at the inlet, pressure outlet at the outlet, periodic boundary condition at the top and at the bottom, wall boundary condition on the airfoil surface. Finer mesh was applied near the airfoil. Viscous model with Realizable k-epsilon (2 equation) turbulence model was chosen.

3.3. Acoustic Model, Assumptions and Corrections

Ffowcs-Williams & Hawkings equation was applied as acoustic model. Convective effects were included since the analysis was dealing with external flow around a body. The explicit formulation which was available only for the density-based solver was utilized mainly to capture the transient behavior of moving waves. While performing transient analysis, acoustic signals were computed simultaneously.

During the calculations time step size was 0.002 seconds, number of time steps was 1000, Max iterations/time step were 50 selected considering stability of the results and convergence. Frequencies of the results were depended on the time step size. Smaller the time step size, higher the frequency range of the sound pressure level.

One of the distinguished aspects of the analysis was applying dynamic angle of attack velocity to the inlet conditions. By applying dynamic angle of attack calculation, horizontal (X) and vertical (Y) components of residual velocity on each blade section were calculated and integrated to the analysis by using User Defined Functions. Incoming wind speed was a step input, then phi angle was calculated; angle of attack (α) was calculated by subtracting twist angle from the flow angle. Resultant velocity, $W(t)$ was determined. Horizontal component of velocity $Wx(t)$ was obtained by multiplying $W(t)$ by cosine of $\alpha(t)$ and similarly, the vertical component $Wy(t)$ was found by multiplying $W(t)$ by sine of $\alpha(t)$.

Unsteady velocity components of x and y directions were calculated and applied as inlet boundary conditions simultaneously through a User Defined Function (UDF).

Selected span wise sections for two-dimensional calculations for comparison were shown in the Figure 1.

Figure 1. Selected Sections For Calculation

Variation of Wx and Wy velocity components with dynamic angle of attack were presented for r/R = 0.47 and r/R =1.0 in Figure 2.

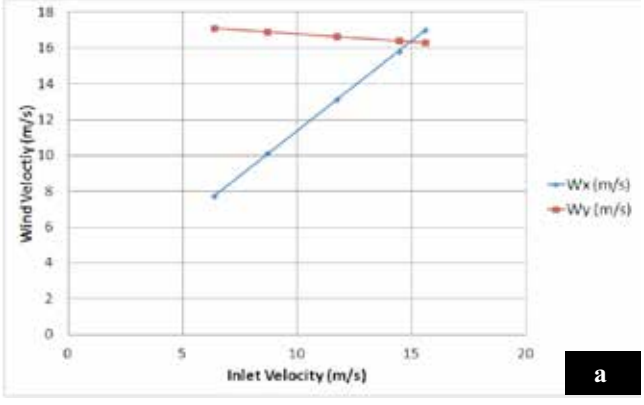

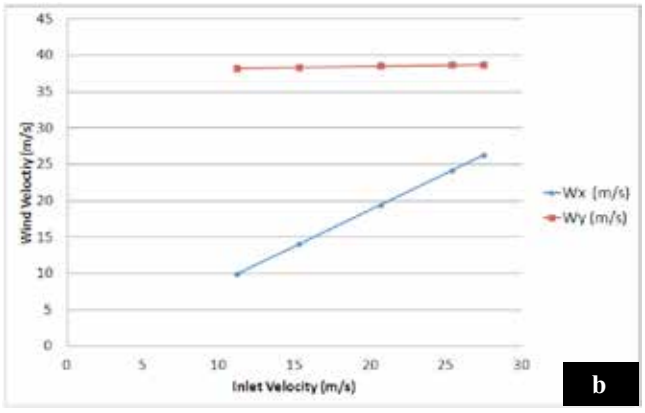

Figure 2. Velocity Variation with Dynamic Angle of Attack at a) r/R=0.47, b) r/R=1.0.

Corrections were made to simulate the two dimensional section noise analysis to blade noise. First correction was to adapt the tapered geometry of blade to 2D section. Reynolds similarity was used to simulate the tapered geometry. Inlet speed kept constant at r/R=0.25, for outer sections inlet speed was corrected to keep the same Reynolds number. Graphical representation was shown in Figure 3.

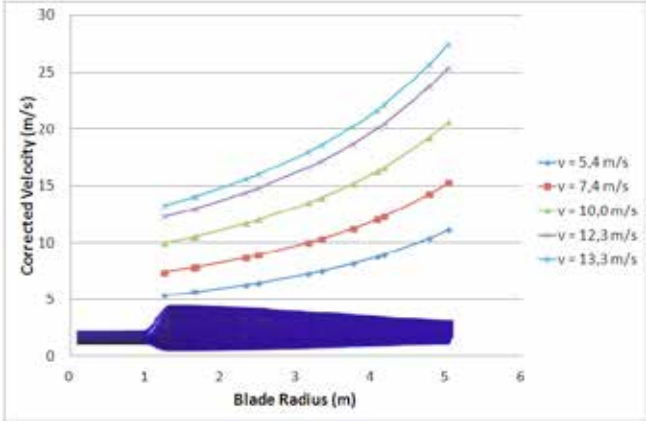

Figure 3. Velocity Correction For Tapered Geometry of the Blade

Second correction was to scale the 2D analysis to 12% scaled model. By using Reynolds similarity, 12% of dynamic viscosity was used to simulate the 12% model test.

$$Re = \frac{\upsilon c}{\nu} \qquad (2)$$

Here, c is the chord length of the airfoil, is the velocity of the fluid and is the kinematic viscosity of the fluid.

Major differences between the three dimensional 12% scaled model test and two dimensional analyses were defined below.

i) In three dimensional (12% scaled) Model Test, actual model noise measurements were performed by using 144 microphones [30].

ii) In two dimensional analysis of the present study;

- Noise of each zone was represented by single two dimensional section noise,
- Single receiver was located 1.88 m away in vertical, 1.49 m away in transversal directions, respectively. These correspond to the coordinates of center of 12% Model Test microphones.
- Interference between sections, tip vortex, and hub vortex effects were not included.

3.4 Sound Power Level vs. Sound Pressure Level

A sound source produces sound power and this generates a sound pressure fluctuation in the air. Where the sound pressure is distance dependent effect, sound power is independent from the distance. Reference values are highly critical for the sound analysis. Reference pressure for sound pressure level (for air) was $2x10^{-5}$ Pascal. Reference power for sound power level was $1x10^{-12}$ Watt.

In order to compare the noise measurements of the study [30] and the two dimensional analysis results, predictions in sound pressure levels (dB) were converted to sound power levels.

The conversion was done by the following formula;

$$L_w = L_p + \left|10\log\left(\frac{Q}{4\pi r^2}\right)\right| \qquad (3)$$

Where L_w is the sound power level, L_p is the sound pressure level and Q is the directivity factor, assumed to be unity for spherical propagation.

3.5 Predicting the Total Noise Of The Blade

First, the blades of the wind turbine were nonuniformly divided into two-dimensional airfoil sections. Then, the summation of the contribution from the each blade section was used to predict the total noise emission [33].

According to the study of Zhu et al. [33], the two dimensional noise prediction theory was applied for each blade section and later on the total noise was determined by summing up all noise sources. The total noise in terms of Sound Pressure Level for the i^{th} blade element was presented in the following formulation [33]:

$$SPL^{i}_{Total} = 10\log_{10}\left(\sum_j 10^{0.1(\mathrm{SPL}_j)}\right) \qquad (4)$$

IV. RESULTS AND DISCUSSION

4.1. Experimental Results for Comparison and Validation

In the study of T.Cho et al., [30] two bladed turbine was rotated at constant rotating speed for wind speeds increasing from 0 to 13 m/s. Array of 144 microphones were installed in circular pattern on the bottom wall of the wind tunnel. The center of the microphones was located 1.88 m away from the turbine center in the downwind direction and 1.49 m in vertical direction toward to the floor [30].

The area around the blade was divided to sequential five zones at different radii as shown in Table 3.

Table 3. Zones of the Blade for Noise Measurements [30]

Zone Description	Boundaries *(r/R)*
A1	0.83 - 1.0
A2	
0.67 - 0.83	
A3	0.50 - 0.67
A4	0.36 - 0.50
A5	0.25 - 0.36

In the study of T. Cho et al., the corresponding noise levels were obtained by using time base beamforming methodology for rotating source. The average source strength for each zone was calculated for specified octave bands. The noise levels were presented as source power level with $1x10^{-12}$ Watt reference power in the study [30] (30) [23].

Average source strengths were presented in the study of T. Cho et al. for wind speeds of 5.4 m/s, 7.4 m/s, 12.3 m/s, and 13.3 m/s at Zone A1 and A2. Graphs were shown as frequency between 1 kHz – 6.3 kHz in X-coordinate and noise power level at dB scale in Y-coordinate [30].

The results were presented in the study of T. Cho et al. for wind speeds of 5.4 m/s, 7.4 m/s, 12.3 m/s, and 13.3 m/s.

In the current work, analyses were performed for Zone A1 and A2 in order to compare and validate the predictions.

4.2. Analysis Results for Zone A1

Zone A1 was defined as the area between $r/R = 0.83$ and $r/R = 1.0$ [30]. Comparison of noise r/R=0.95 and 1.0 for Zone A1 at 5.4 m/s wind velocity were presented in Figure 4.

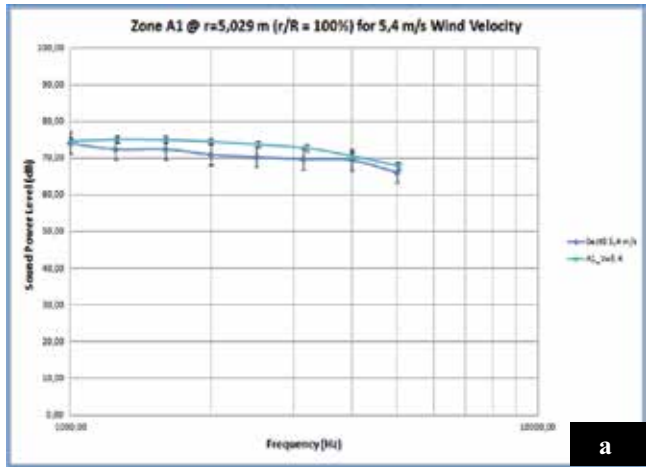

Min Err= 1.80 dB, Max Err= 5.43 dB

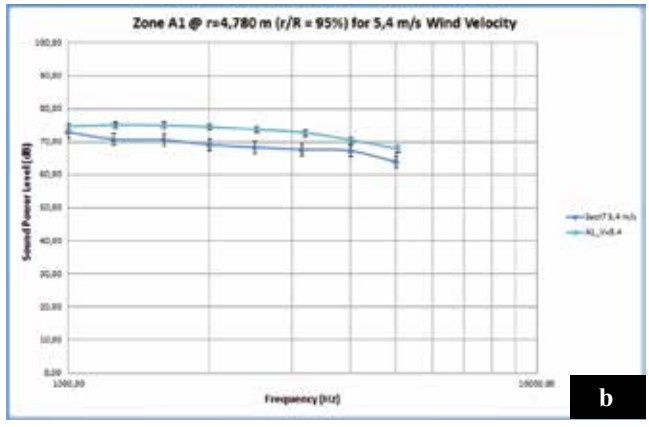

Min Err= 0.66 dB, Max Err= 3.59 dB

Figure 4. SPL (dB) for 5.4 m/s at a) r/R=0.95, b) r/R=1.0.

General trend of the predictions has agreed well with the measurements. Difference increased about 1 dB for inner section. By combining previous results, following noise graph at 5.4 m/s for Zone A1 was calculated and displayed in Figure 5.

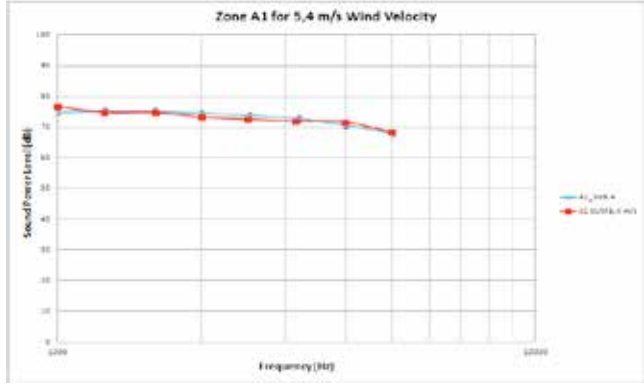

Figure 5. Comparison of Section Noise for Zone A1 at 5.4 m/s

Noise of the airfoil in the tip region was predicted fairly well at 5.4 m/s. The analysis results were in very good agreement with the experimental results for lower wind speeds.

Comparison of noise r/R=0.95 and 1.0 for Zone A1 at 7.4 m/s wind velocity were presented in Figure 6. Predictions agreed well with the measurements except at 1.25 kHz and 2.0 kHz frequencies. Predictions underestimated the measurements about 6 – 11 dB at r/R=0.95 section, 8 - 13 dB at r/R=1.0 section. After combining previous results, following noise graph at 7.4 m/s for Zone A1 was calculated and displayed in Figure 7.

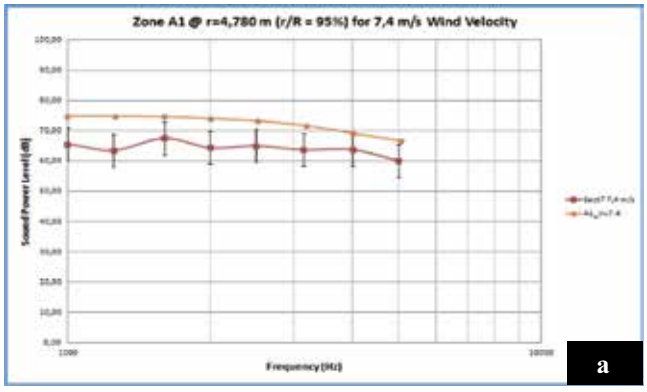

Min Err= 5.41 dB, Max Err= 11.27 dB

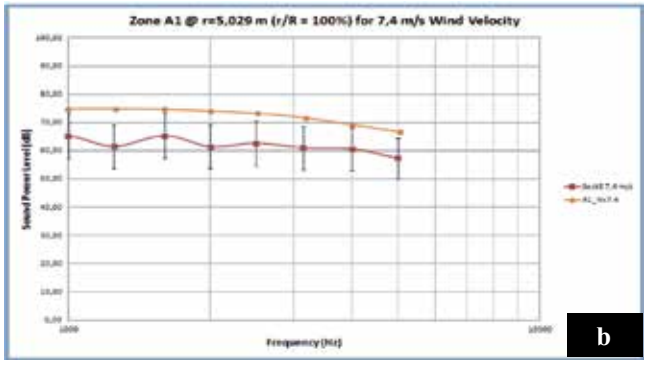

Min Err= 8.65 dB, Max Err= 13.33 dB

Figure 6. SPL (dB) for 7.4 m/s at a) r/R=0.95, b) r/R=1.0

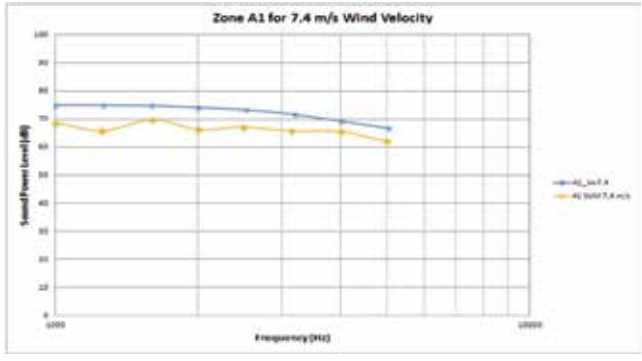

Figure 7. Comparison of Section Noise for Zone A1 at 7.4 m/s

Predictions underestimated the measurements about 5 – 7 dB through the Zone A1. It was believed that this might be due to laminar-turbulent transition which occurs in actual flow but neglected in the computations.

SPL predictions for Zone A1 at 12.3 m/s wind velocity were presented in Figure 8.

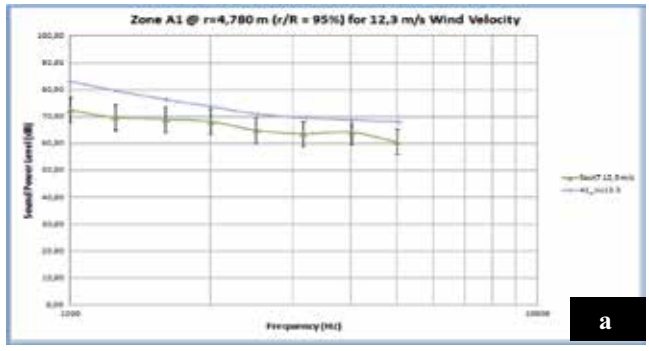

Min Err= 4.66 dB, Max Err= 10.68 dB

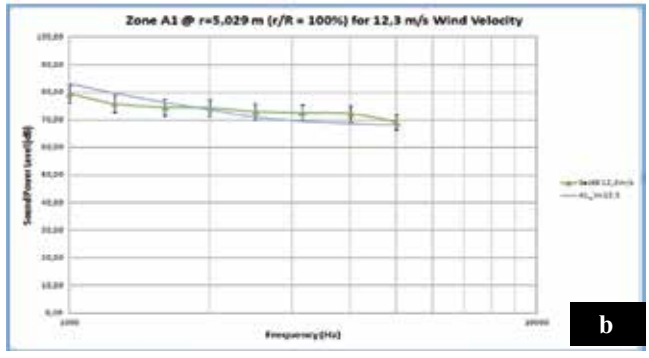

Min Err= 0.51 dB, Max Err= 3.83 dB

Figure 8. SPL (dB) for 12.3 m/s at a) r/R=0.95, b) r/R=1.0

For r/R=1.0 section, computations underestimated the SPL until 2.0 kHz and overestimated it between 2.0 - 4.0 kHz. But less than 4 dB difference for all frequency band was observed.

Similarly, the combined noise graph at 12.3 m/s for Zone A1 was shown in Figure 9.

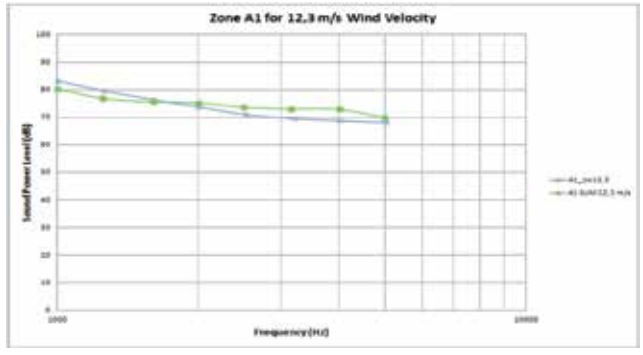

Figure 9. Comparison of Section Noise for Zone A1 at 12.3 m/s

For Zone A1, noise of the airfoil in the tip region was predicted fairly well at 12.3 m/s. Maximum deviation was around 3 dB in all frequency band.

Predictions for Zone A1 at 13.3 m/s wind velocity were presented in Figure 10.

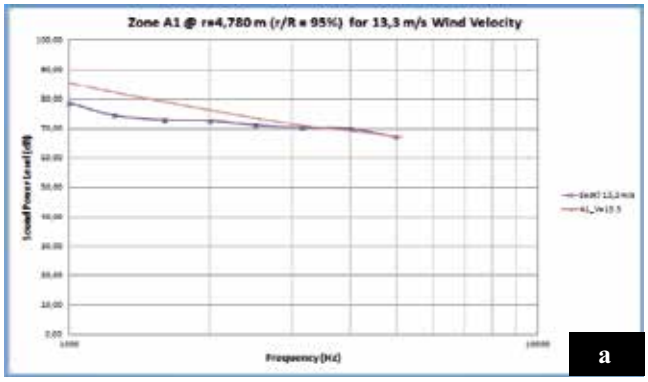

Min Err= 0.47 dB, Max Err= 7.86 dB

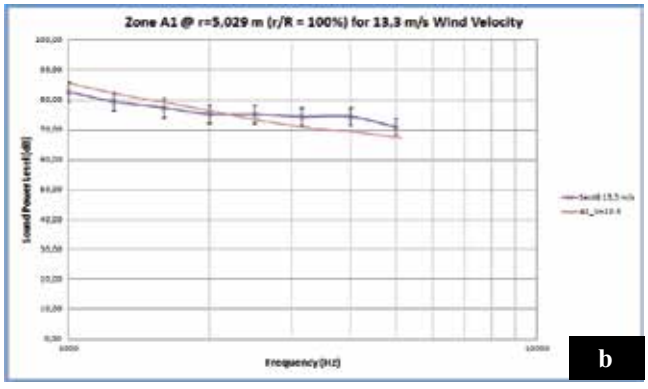

Min Err= 1.09 dB, Max Err= 5.09 dB

Figure 10. SPL (dB) for 13.3 m/s at a) r/R=0.95, b) r/R=1.0

For *r*/*R*=1.0 section, predictions were agreed well until 2.0 kHz frequency, above this frequency the predictions were overestimated the measurements. But less than 5 dB difference for all frequency band was observed. For *r*/*R*=0.95 section, predictions were in very good agreement with measurements at high frequencies but they underestimated SPL at lower ones.

The combined noise graph at 13.3 m/s for Zone A1 was calculated and presented in figure 11. At 13.3 m/s, predictions were fitted well to the measurements until 2.0 kHz frequency. Above this frequency the analysis results were overestimated the measurements. However, above 2.0 kHz frequency, maximum difference between the computations and measurements was about 5 dB and average difference between them was about 3 dB.

Overall, for Zone A1, the agreement between predictions and measurements was best at 5.4 m/s and worst for 7.4 m/s wind speed. At higher wind speeds, computations predicted SPL with reasonable accuracy at lower frequencies. However, for all wind speeds, SPL difference between computations and measurements remained less than approximately 7 dB.

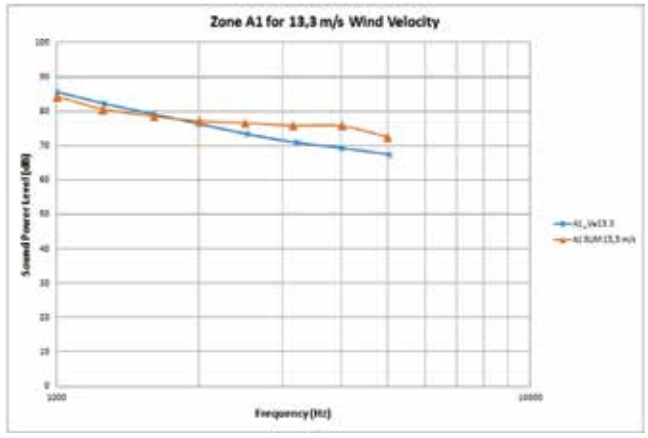

Figure11. Comparison of Section Noise for Zone A1 at 13.3 m/s

4.3. Analysis Results for Zone A2

Zone A2 was defined as the area between *r*/*R* = 0.67 and *r*/*R* = 0.83 [30]. SPL predictions were obtained at wind speeds of 5.4, 7.4, 12.3 and 13.3 m/s and compared with the corresponding wind tunnel measurements [30]. Similar to the analyses performed for Zone A1, SPL predictions were first obtained at two radial stations in the zone and then they were combined to obtain an SPL prediction for the whole zone.

SPL predictions at *r*/*R*=0.75 and 0.81 at 5.4 m/s wind velocity were presented and compared with measurements Figure 12. For both stations, computations underestimated the SPL. However, numerical results obtained for these two stations turned out to be almost same unlike predictions represented in the previous section. This behavior emphasizes the redundancy of analysis for this zone.

Combined SPL predictions and corresponding wind tunnel measurements for 5.4 m/s wind speed were displayed in Figure 13. Predictions and measurements were agreed well within the 1.0 - 1.25 kHz band. However, at higher frequencies the computations were underestimated SPL values. The maximum and average difference between predictions and measurements was about 6 dB and 4 dB within the 1.25 - 4.0 kHz band, respectively.

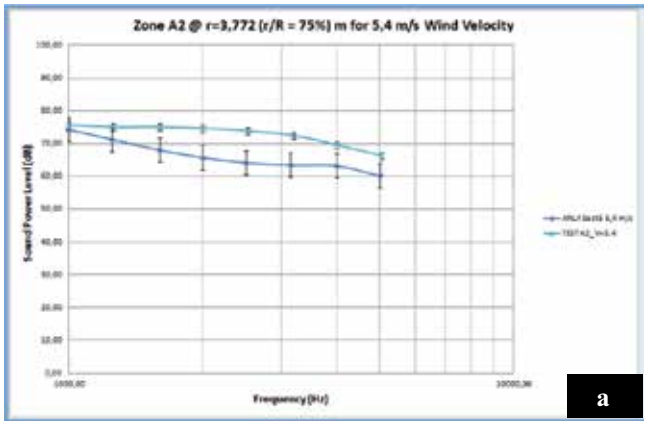

Min Err= 1.45 dB, Max Err= 9.36 dB

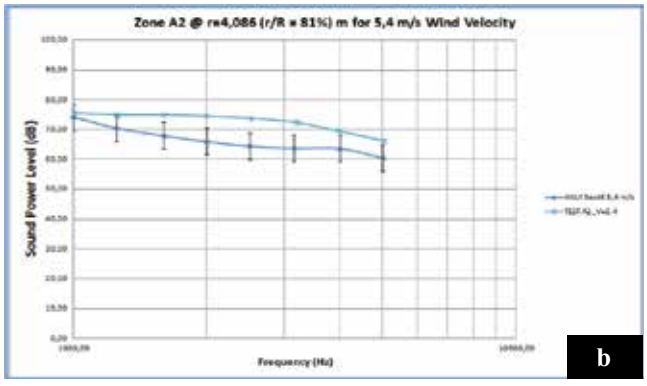

Min Err= 1.40 dB, Max Err= 9.57 dB

Figure 12. SPL (dB) for 5.4 m/s at a) r/R=0.75, b) r/R=0.81

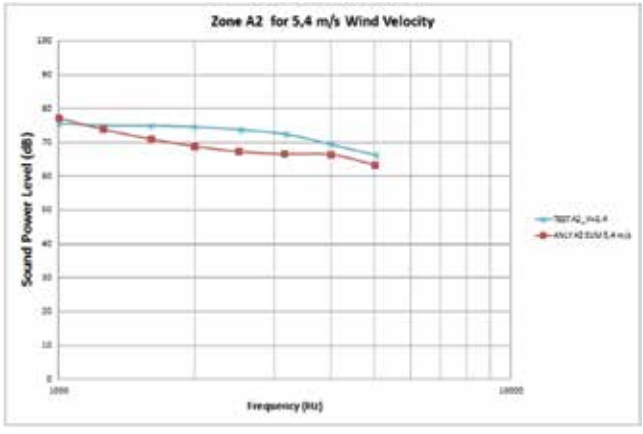

Figure 13. Comparison of Section Noise for Zone A2 at 5.4 m/s

Local and combined SPL predictions obtained at 7.4 m/s were displayed in Figure 14 and Figure 15, respectively. Similar the 5.4 m/s case, numerical predictions obtained for both radial stations were almost same. However, unlike the results obtained for Zone A1, the predictions for this zone were relatively in better agreement with the experiment at this wind speed.

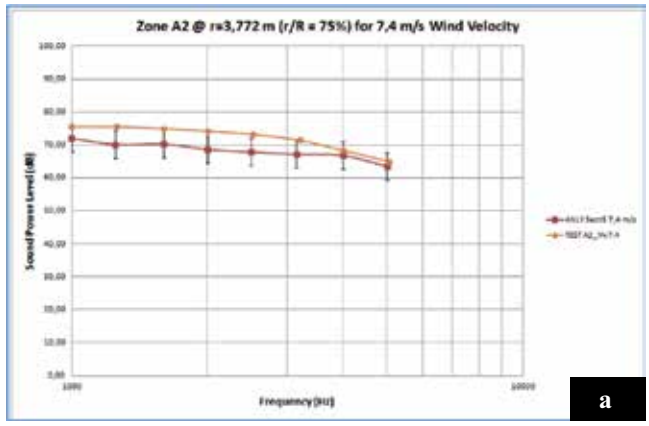

Min Err= 0.21 dB, Max Err= 5.09 dB

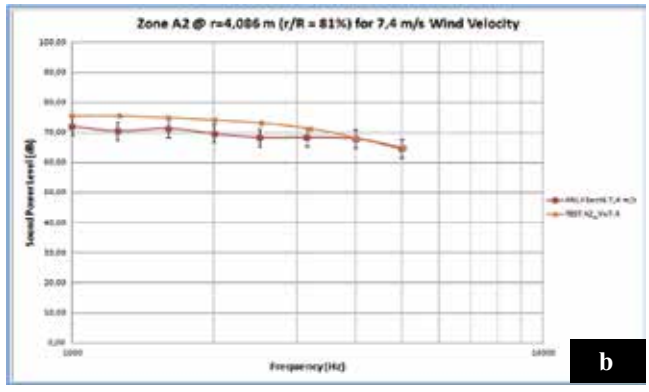

Min Err= 1.33 dB, Max Err= 5.52 dB

Figure 14. Comparison of Section Noise for Zone A2 at 7.4 m/s

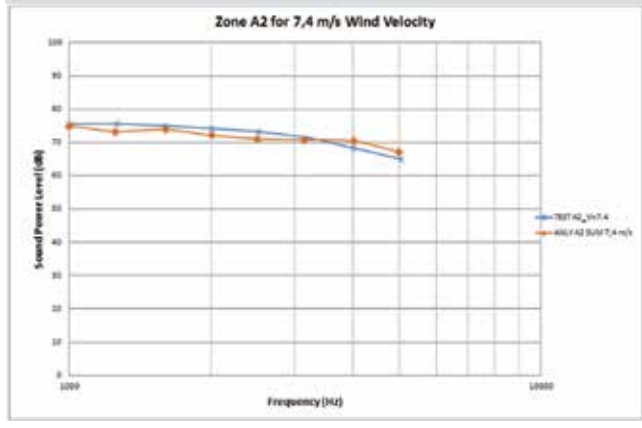

Figure 15. SPL (dB) for 7.4 m/s at a) r/R=0.75, b) r/R=0.81

Figure 16 and Figure 17 display the local and combined SPL predictions obtained at 12.3 m/s wind speed, respectively. It was clear from Figure 15 that, as the wind speed increased the effect of the location of the radial station on the predictions became more distinct. The overall predictions underestimated the SPL values about 10 – 12 dB at all frequencies. However, computations were able to predict the slope of the curve fairly accurately.

Finally, local and combined SPL predictions obtained at 13.3 m/s were displayed in Figure 18 and Figure 19, respectively. Predictions obtained in this wind speed were similar to those obtained for 12.3 m/s. Here, computations underestimated the measurements about 14 – 18 dB for the frequency band but again they were able to compute the general trend of the curve fairly accurately. It was evaluated that methodology could provide reasonable results even in higher wind speeds based on the accurate prediction of the slope of the curve.

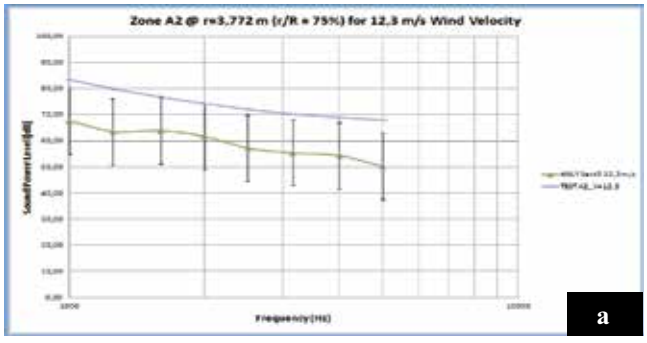

Min Err= 12.52 dB, Max Err= 17.59 dB

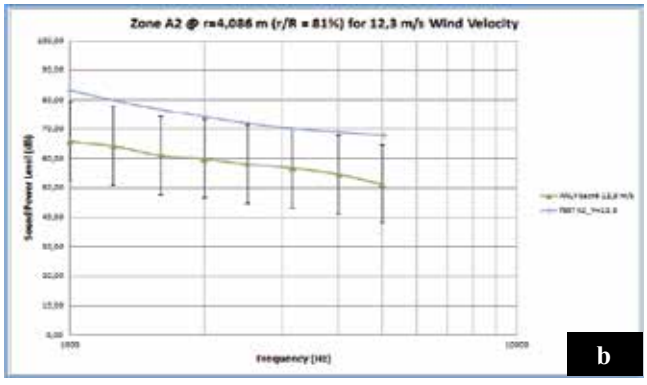

Min Err= 13.30 dB, Max Err= 17.32 dB

Figure 16. SPL (dB) for 12.3 m/s at a) r/R=0.75, b) r/R=0.81

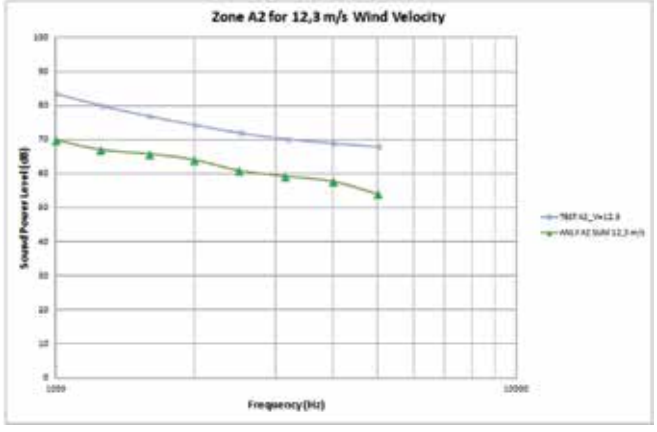

Figure 17. Comparison of Section Noise for Zone A2 at 12.3 m/s

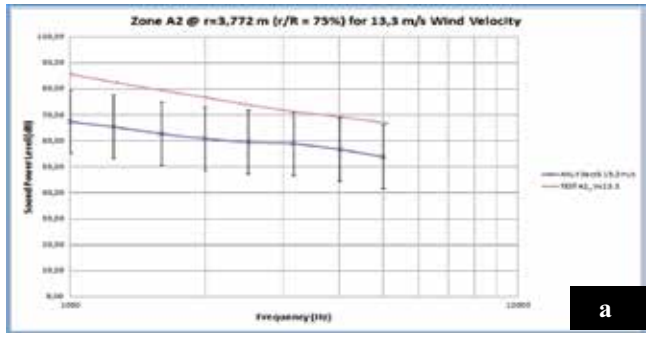

Min Err= 12.05 dB, Max Err= 17.90 dB

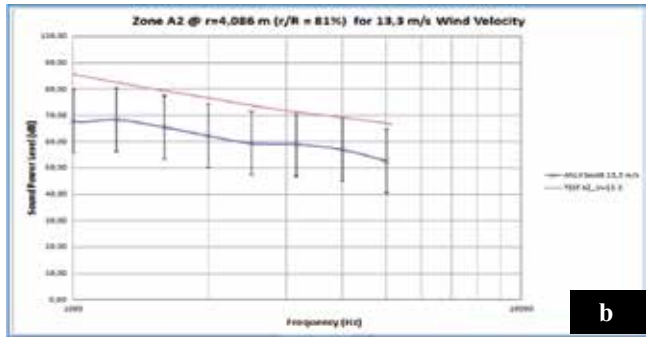

Min Err= 12.19 dB, Max Err= 18.25 dB

Figure 18. SPL (dB) for 13.3 m/s at a) r/R=0.75, b) r/R=0.81

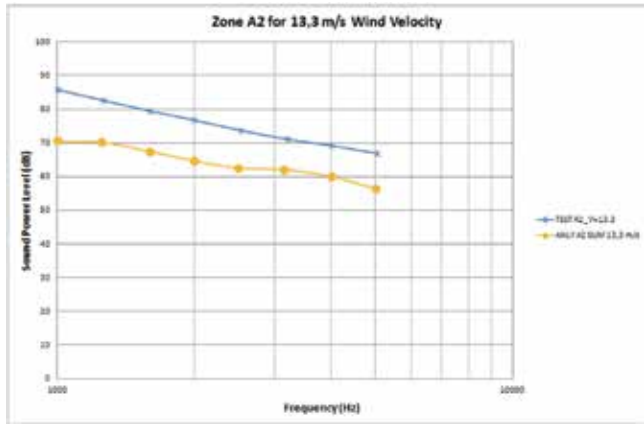

Figure 19. Comparison of Section Noise for Zone A2 at 13.3 m/s

Considering the comparisons between predictions and measurements presented above, it can be concluded that the two dimensional model employed in this study could predict the noise generated by the turbine blade with reasonable accuracy at low wind speeds like 5.4 m/s although it does not take into account the interactions between the sections two-dimensional sections. As the wind speed increased however, the quality of the predictions were affected by the zone in consideration. Therefore, this two-dimensional model tested

in this study can be used with reasonable confidence to predict noise generated by wind turbines at low wind speeds where the flow is mainly attached to the blades. Considering the fact that the wind turbines that would be placed in urban areas would have to operate at low wind speeds [34,35], the model can be considered as a valuable tool to design and optimize wind turbines for lower noise generation.

Additionally, the decay of the residuals for iterations was presented in Figure 20.

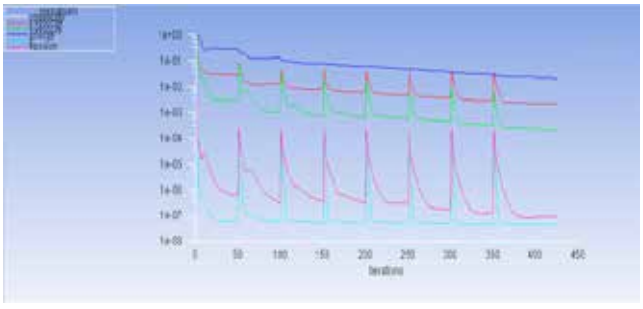

Figure 20. The Decay of the Residuals

4.4 Prediction of The Blade Noise

The summation of the contribution from the each blade section was used to predict the total noise emission by using following formulation [33].

$$SPL^{i}_{Total} = 10\log_{10}\left(\sum_{j} 10^{0.1(\mathrm{SPL}_j)}\right) \quad (4)$$

The total noise generated by the blade (comprised of S809 airfoil sections) at different wind speeds was presented in Figure 21. According to the figure the hub and the tip regions of the blade generated more noise compared to the intermediate spanwise locations. Therefore, the design of these sections can be said to be more critical to obtain quieter blades.

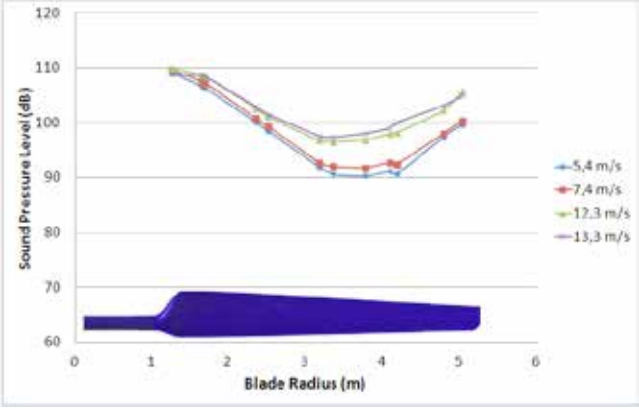

Figure 21. Prediction of the Blade Noise

V. CONCLUSIONS

In order to compare the generated noise of the %12 scaled model of the NREL Phase VI wind turbine with the analysis results, certain steps were applied.

First, relative velocity components (*Wx* and *Wy*) were calculated simultaneously for each section by using UDFs. Secondly, tapered geometry of actual blade was simulated by keeping the Reynolds number constant to be able to utilized the current mesh. Third, 12% dynamic viscosity was used to simulate the 12% scaled model. And finally, calculated Sound Pressure Levels (dB) were converted to Sound Power Levels (dB) to compare the measurements and analysis results.

The summary of the results;

For tip area (Zone A1), noise analysis at 5.4 m/s wind speed showed good agreement with the model measurements in terms of trend and magnitude. At higher wind speeds the quality of the predictions was degraded however the difference between predictions and measurement did not exceed 7 dB in the frequency range considered.

For inboard area (Zone A2) noise predictions were also in good agreement with measurements at low wind speeds, especially at 7.4 m/s. However, at higher wind speeds the computations underestimated the SPL considerably while predicting the general trend of the SPL vs. frequency curve reasonably accurately.

Considering the comparisons made at different zones and wind speeds, it was concluded that the two-dimensional model used in this study can be used to predict the noise level of wind turbine blades with reasonable accuracy at low wind speeds.

Additionally, overall SPLs of the whole blade were calculated at 1.88 m away along the blade sections. Higher SPLs were observed around tip and chub regions compared to the mid sections of the blade. These sections may be critical while optimizing the blade geometry for low noise emission.

REFERENCES

[1] Fried, L., Qiao, L., Sawyer, S., Shukla, S. “Global Wind Report – Annual Market Update 2014” GWEC, Global Wind Energy Council, Brussels, Belgium, 2014.

[2] EREC, European Renewable Energy Council. “Renewable Energy Technology Roadmap 20% by 2020” Renewable Energy House, Brussels, Belgium, 2008.

[3] Rogers, A.L., Manwell, J.F., Wright, S. “Wind Turbine Acoustic Noise” Renewable Energy Research Laboratory, Department of Mechanical and Industrial Engineering

University of Massachusetts at Amherst, Amended 2006.

[4] Gipe, P. "Wind Energy Comes of Age", John Wiley & Sons, Ltd, Chichester, 1995.

[5] Koppen, E., Fowler, K. "International Wind Turbine Noise Legislation Illustrated by a Cross Border Case Study" EWEA Workshop Wind Turbine Sound, 2014.

[6] Pedersen, E., Waye, K.P. "Perception and annoyance due to wind turbine noise - a dose response relationship" Journal of Acoustical Society of America, Vol. 116, No. 6, pp. 3460–3470, December 2004.

[7] Van Den Berg, G.P. "Effects of the wind profile at night on wind turbine sound" Journal of Sound and Vibration 277, pp. 955–970, 2004.

[8] Nissenbaum, M.A., Aramini, J.J., Hanning, C.D. "Effects of industrial wind turbine noise on sleep and health" Noise & Health, September - October 2012, Volume 14, pp. 237-243, 2012.

[9] Council of Canadian Academies. "Understanding the Evidence: Wind Turbine Noise. Ottawa (ON): The Expert Panel on Wind Turbine Noise and Human Health" Council of Canadian Academies, 2015.

[10] Schmidt, J.H., Klokker, M. "Health Effects Related to Wind Turbine Noise Exposure: A Systematic Review" PLoS ONE 9(12):e114183, 2014.

[11] Onakpoya, I.J., O'Sullivan, J., Thompson, M.J., Heneghan, C.J. " The effect of wind turbine noise on sleep and quality of life: A systematic review and meta-analysis of observational studies" Environment International 82, pp. 1-9, 2015.

[12] Son, E., Kim, H., Kim, H., Choi, W., Lee, S. "Integrated numerical method for the prediction of wind turbine noise and the long range propagation" Current Applied Physics 10, pp. 316-319, 2010.

[13] Guarnaccia, C., Mastorakis, N.E., Quartieri, J. "A mathematical approach for wind turbine noise propagation" Proceedings of the 2011 American Conference on Applied Mathematics and the 5th WSEAS International Conference on Computer Engineering and Applications, pp. 187-194, 2011.

[14] Tadamasa, A., Zangeneh, M. "Numerical prediction of wind turbine noise" Renewable Energy 36, pp.1902-1912, 2011.

[15] Leishman, J.G. "Challenges in Modeling the Unsteady Aerodynamics of Wind Turbines" Wind Energy 5, pp. 85 - 132, 2002.

[16] Simms, D., Schreck, S., Hand, M., Fingersh, L.J. "NREL Unsteady Aerodynamics Experiment in the NASA-Ames Wind Tunnel: A Comparison of Predictions to Measurements" NREL/TP-500-29494, National Renewable Energy Laboratory, 2001.

[17] Katinas, V., Marciukaitis, M., Tamasauskiene, M. "Analysis of the wind turbine noise emissions and impact on environment" Renewable and Sustainable Energy Reviews 58, pp. 825-831, 2016.

[18] Göçmen, T., Özerdem, B. "Airfoil optimization for noise emission problem and aerodynamic performance criterion on small scale wind turbines" Energy 46, pp. 62-71, 2012.

[19] Lee, S., Lee S. "Numerical and experimental study of aerodynamic noise by a small wind turbine" Renewable Energy 65 , pp. 108-112, 2014.

[20] Ramirez, W.A., Wolf, W.R. "Effects of trailing edge bluntness on airfoil tonal noise at low Reynolds numbers" Journal of Brazilian Society of Mechanical Sciences and Engineering, 2015.

[21] Lighthill, M.J. "On Sound generated aerodynamically I. General theory" Proceedings of the Royal Society of London. Series A, Mathematical and Physical Sciences, pp.564-587, 1951.

[22] Ffowcs Williams J.E., Hawkings D.L. "Sound generation by turbulence and surfaces in arbitrary motion" Philosophical Transactions of the Royal Society of London. Series A, Mathematical and Physical Sciences, Vol. 264, No. 1151, pp. 321-342, 1969.

[23] Brentner, S.K., and Farassat, F. "Modeling aerodynamically generated sound of helicopter rotors" Progress in Aerospace Sciences 39, pp.82-120, 2003.

[24] Tadamasa, A., Zangeneh, M. "Numerical prediction of wind turbine noise" Renewable Energy 36, pp.1902-1912, 2011.

[25] Filios, A.E, Tachos, N.S., Fragias, A.P., Margaris, D.P. "Broadband noise radiation analysis for an HAWT rotor" Renewable Energy 32, pp. 1497-1510, 2007.

[26] Di Francescantonio, P. "A new boundary integral formulation for the prediction of sound radiation" Journal of Sound and Vibration 202(4), pp.491-509, 1997.

[27] Brentner, K.S., Farassat, F. "An analytical comparison of the acoustic analogy and Kirchhoff formulation for moving surfaces" AIAA Journal 36, no.8, pp.1379-1386, 1998.

[28] Rahier, G., Huet, M., Prieur, J. "Additional terms for the use of Ffowcs Williams and Hawkings surface integrals in turbulent flows" Computer and Fluids 120, pp. 158-172, 2015.

[29] Hand, M., Simms, D., Fingersh, L., Jager, D., Cotrell, J., Schreck, S., Larwood, S. "Unsteady Aerodynamics Experiment Phase VI: Wind Tunnel Test Configurations and Available Data Campaigns," NREL/TP-500-29955, National Renewable Energy Laboratory, 2001.

[30] Cho, T., Kim,C., Lee,D. "Acoustic measurement for 12% scaled model of NREL Phase VI wind turbine by using beamforming" Korea Aerospace Research Institute, Daejeon 305-333, Current Applied Physics 10, pp. 320 – 325, 2010.

[31] ANSYS Inc., Release 14.0, ANSYS FLUENT User's Guide, 2011.

[32] Somers, D.M. "Design and Experimental Results for the S809 Airfoil" NREL/SR-440-6918, National Renewable Energy Laboratory, 1997.

[33] Zhu, W.J., Heilskov, N., Shen W.Z., Sorensen, J.N. "Modeling of Aerodynamically Generated Noise From Wind Turbines" Journal of Solar Engineering, Vol 127/527, 2005.

[34] Cace, J., ter Horst, E., Sybgellakis, K., Niel, M., Clement, P., Heppener, R., Peirano, E., "Urban Wind Turbines: Guidelines for Wind Turbines for the Built Environment" Wineur Report, 2007.

[35] Kaldellis, J.K., Zafirakis, D., Kondili, E., Papapostolou, Chr. "Trends, Prospects and R&D Directions of the Global Wind Energy Sector" Proceedings of EWEA 2012 Annual Event, April 2012.